International Journal of GEOMATE
(Geotechnique, Construction Materials and Environment)
ISSN: 2186-2982 (P), 2186-2990 (O), Japan
Vol. 31, Issue 145, September 2026, PP.141-155; DOI: 10.21660/2026.145.5690

CALIBRATION OF CONVERSE-LABARRE EQUATION FOR BORED PILE GROUPS IN BANGKOK SUBSOIL USING 3D FEM

Nitirach Sa-nguanduan[1] and *Kamol Amornfa[2]

[1]Department of Irrigation Engineering, Faculty of Engineering at Kamphaeng Saen, Kasetsart University, Thailand; [2]Department of Civil Engineering, Faculty of Engineering at Kamphaeng Saen, Kasetsart University, Thailand

*Corresponding Author, Received: 27 May 2026, Revised: 24 June 2026, Accepted: 19 June 2026

ABSTRACT: Conventional pile-group efficiency equations are used widely in foundation design; however, their applicability remains uncertain to bored pile groups in Bangkok soft clay, because simplified formulations do not account explicitly for soil-dependent pile-soil-pile interactions. This study evaluated and calibrated the Converse-Labarre equation for Bangkok subsoil using three-dimensional finite element analyses (3D FEM). Two representative bored pile series were considered: a smaller pile terminating in the first sand layer and a larger pile extending to the second sand layer. Pile-group efficiency was interpreted from FEM-derived load-settlement curves using the Chin method, with the Mazurkiewicz method used as an independent graphical check. The results showed that FEM-derived efficiency was consistently lower than unity, decreasing with an increasing number of piles, and increasing with an increasing spacing ratio. Among the classical capacity-based methods considered, the Converse-Labarre equation better captured the effects of both pile number and spacing ratio, although further correction was needed, especially at close spacing. Therefore, a Bangkok-specific correction factor was developed as a multiplicative adjustment to the original Converse-Labarre efficiency, with regression terms based on $\ln(n)$ and $1/\ln(s/D)$. The selected model had R^2 = 0.587, reduced the mean absolute error from 3.46% to 2.61%, and reduced the maximum absolute error from 19.53% to 12.03%. The proposed correction preserves the simplicity of the Converse-Labarre equation and provides geotechnical engineers with a practical preliminary adjustment for estimating bored pile-group efficiency in Bangkok subsoil.

Keywords: Bored Pile Group; Converse-Labarre Equation; Bangkok Subsoil; Finite Element Analysis; Pile Group Efficiency

1. INTRODUCTION

The design of pile groups in soft clay involves complex soil-structure interaction mechanisms that greatly influence the foundation load-settlement response. Commonly, in conventional practice, the ultimate capacity of a pile group is estimated as the sum of the individual pile capacities multiplied by a group-efficiency factor (η). Among the available empirical methods, the Converse-Labarre equation has been used widely, because of its simplicity and dependence on pile spacing and group geometry [1]. However, this formulation does not account explicitly for soil-dependent behavior, stress overlap, or nonlinear deformation. According to the American Society of Civil Engineers (ASCE) guidelines, group-efficiency correction is required for friction piles in cohesive soils and for piles in granular soils with spacing less than three times the pile diameter [2]. This issue is particularly relevant to Bangkok, where bored piles commonly behave as friction piles embedded in thick, highly compressible soft clay. Under such conditions, interaction zones between adjacent piles may overlap, reducing group efficiency even at moderate spacing ratios; similar behavior has been reported for friction pile groups in soft soils [3, 4].

Current foundation design practice in Bangkok still relies largely on simplified analytical methods that cannot fully represent three-dimensional pile-soil-pile interactions and the influence of stratified soft-clay deposits [5]. In contrast, 3D FEM analyses have been used increasingly to evaluate load transfer, settlement distribution, and load redistribution within pile and piled foundation systems [6–10]. In addition, previous experimental, field, and numerical studies have shown that conventional pile-group efficiency equations may not consistently capture pile-soil-pile interactions because the pile spacing, group size, soil behavior, and stress-field interaction are not fully represented in simplified empirical formulations [3, 11, 12]. These findings indicated the need for soil-specific evaluation of pile-group efficiency in highly compressible clay deposits.

Despite the continued use of the Converse-Labarre method in routine foundation design, this equation has not yet been calibrated systematically for bored pile groups in Bangkok soft clay. The present study addressed this gap by performing three-dimensional FEM analyses of bored pile groups in representative Bangkok subsoil, comparing the numerical results with classical efficiency formulations and developing a Bangkok-specific correction factor for the Converse-Labarre equation. The proposed approach aimed to preserve the practical simplicity of the original method while improving its agreement with FEM-derived pile-group efficiency under local subsoil conditions.

2. RESEARCH SIGNIFICANCE

This study provides a soil-specific evaluation of bored pile-group efficiency in Bangkok soft clay using three-dimensional FEM analyses based on representative local subsoil parameters. By comparing FEM-derived efficiencies with classical empirical methods, the study clarifies the applicability and limitations of the Converse-Labarre equation under Bangkok conditions. The proposed correction factor improves practical estimation, while preserving the simplicity required for routine design. The findings support more rational and economical foundation design for high-rise buildings in Bangkok and provide a basis for further calibration using field data.

3. REVIEW OF EFFICIENCY METHODS

The concept of pile-group efficiency (η) is used commonly to express the deviation of pile-group capacity from the sum of the capacities of individual piles. Generally, classical efficiency methods estimate this effect using simplified relationships based on pile arrangement, spacing, and group geometry. Among these methods, the Converse-Labarre equation remains one of the most widely used because of its simplicity and ease of application [1]. For a rectangular pile group, the efficiency may be expressed as:

$$\eta_{CL} = 1 - \frac{\theta}{90^\circ}\left[\frac{(c-1)r+(r-1)c}{rc}\right] \quad (1)$$

where η_{CL} is the pile-group efficiency, r is the number of rows, c is the number of columns, and θ is $\tan^{-1}(D/s)$ in degrees, with D denoting the pile diameter and s the center-to-center pile spacing, and $n = rc$ is the total number of piles in the group.

Although convenient for routine design, the Converse-Labarre equation is essentially geometric and does not account explicitly for soil-dependent interaction mechanisms such as stress overlap, compressibility, and nonlinear deformation.

Several alternative methods have been proposed to improve or simplify the estimation of pile-group efficiency. Feld introduced a rule-of-thumb approach in which the capacity of a pile group is reduced according to the number of adjacent pile interactions [13]. Whitaker proposed experimental design charts for evaluating pile-group efficiency [14], while Seiler and Keeney developed an empirical expression incorporating spacing and group arrangement effects [15]. Later, Sayed and Bakeer proposed a formula that considered three-dimensional group geometry, shaft-load contribution, soil characteristics, friction factors, and group-interaction effects [16]. More recent developments have included settlement-based approaches and data-driven models such as the method of McCabe and Lehane and the artificial neural network model of Hanna, Morcous, and Helmy [17, 18].

Recent numerical and experimental studies further indicate that pile-group efficiency is affected strongly by soil condition, pile type, installation method, spacing, and group configuration. Ferchat, Houhou, and Benmebarek performed three-dimensional FLAC3D analyses of pile groups in soft clay and found that generally, efficiency was lower than unity and strongly influenced by pile spacing and group size [11]. Pratama, Widjaja, and Budianto used three-dimensional FEM analyses for pile groups in cohesive, cohesionless, and stratified soils and showed that empirical formulas may either overestimate or underestimate numerical efficiencies depending on the soil type and configuration [12]. Additional recent studies on driven piles, bored piles, numerical pile-group models, and composite pile groups have shown that efficiency can vary substantially with pile spacing, pile number, pile diameter, relative density, cap condition, and soil profile [19–22].

Overall, the reviewed literature showed that classical efficiency equations remain useful for routine design; however, their applicability may be limited when a pile-soil-pile interaction is governed by local soil behavior and three-dimensional stress redistribution. These limitations support the use of three-dimensional numerical analyses to reassess pile-group efficiency under conditions representative of Bangkok subsoil. The following section describes the methodology adopted in this study, including numerical model development, material parameter selection, loading procedure, and parametric analysis.

4. METHODOLOGY

The research workflow consisted of: (1) selecting representative Bangkok subsoil and bored pile series; (2) developing and benchmarking the 3D FEM model; (3) conducting parametric analyses of pile number and spacing ratio; (4) interpreting pile capacities; (5) comparing classical efficiency equations; and (6) developing and assessing the Bangkok correction factor.

4.1 Overview of Numerical Framework and Parametric Matrix

Three-dimensional finite element method (FEM) analyses were conducted using PLAXIS 3D to evaluate the efficiency of bored pile groups embedded in Bangkok subsoil under vertical loading. The numerical framework explicitly modelled individual piles and the surrounding soil to capture pile-soil-pile interactions associated with nonlinear soil deformation, stress redistribution, pile spacing, and group configuration. The analyses focused on the short-term response of the clay-dominated Bangkok subsoil profile, in which the clay layers were modelled under undrained conditions and the sand layers were modelled as drained materials.

A consistent modelling approach was adopted for all cases to ensure comparability of the FEM-derived group efficiencies. The parametric study considered two main variables: the number of piles in the group, expressed as *n*, and the spacing ratio, expressed as s/D, where s is the center-to-center pile spacing and D is the pile diameter. Two representative bored pile series were used to reflect typical foundation scales in Bangkok practice. The smaller pile series, with D = 0.5 m and L = 26 m, represents bored piles terminating in the first sand layer, whereas the larger pile series, with D = 1.0 m and L = 46 m, represents bored piles extending to the second sand layer.

The analyzed cases consisted of single-pile reference models, pile groups with varying numbers of piles at s/D = 3, and nine-pile groups with varying spacing ratios. These cases are summarized in Tables 1–3, and the representative Bangkok subsoil profile with the two different pile series is shown in Fig.1. This framework allowed the effects of pile number and spacing ratio to be evaluated separately under consistent soil conditions and modelling assumptions, providing the basis for comparison with classical efficiency methods and for subsequent development of a Bangkok-specific correction factor. The larger spacing ratios in the nine-pile series were included to examine the convergence of pile-group efficiency toward isolated-pile behavior and should be interpreted as part of the parametric study rather than as a recommendation for routine pile layout.

Table 1. Single-pile reference cases

Case	*D* (m)	*L* (m)	*n*
Smaller pile	0.5	26	1
Larger pile	1.0	46	1

Table 2. Pile-number variation at s/D = 3

Series	*D* (m)	*L* (m)	*s/D*	*n*
Smaller pile	0.5	26	3	2, 4, 9, 16, 25, 36, 49, 64, 81
Larger pile	1.0	46	3	2, 4, 9, 16, 25, 36, 49, 64, 81

Note: The two-pile case was modelled as a linear 1×2 arrangement. For n ≥ 4, square pile-group arrangements were used, ranging from 2×2 to 9×9.

Table 3. Spacing-ratio variation for nine-pile groups

Series	*D* (m)	*L* (m)	*n*	*s/D*
Smaller pile	0.5	26	9	2, 3, 4, 5, 6, 7, 8, 9, 10
Larger pile	1.0	46	9	2, 3, 4, 5, 6, 7, 8, 9, 10

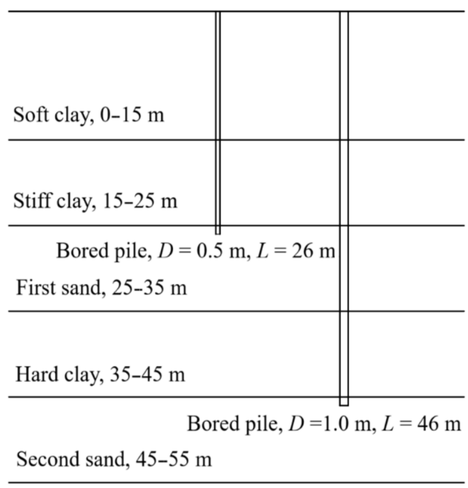

Fig.1 Representative Bangkok subsoil profile and bored pile series used in FEM analyses.

Table 4. Adopted Bangkok subsoil parameters for FEM analyses

Soil parameter	Soft clay	Stiff clay	1st Sand	Hard clay	2nd Sand
Material model	HS	HS	MC	HS	MC
Drain condition	Undrained B	Undrained B	Drained	Undrained B	Drained
Depth (m)	0–15	15–25	25–35	35–45	45–55
γ (kN/m^3)	15.2	18.4	19.4	19.8	20.1
E_{50}^{ref} (MPa)	10	180	-	600	-
E_{oed}^{ref}(MPa)	10	180	-	600	-
E_{ur}^{ref} (MPa)	30	540	-	1,800	-
$E^{'}$ (MPa)	-	-	4,500	-	7,000
m	1	1	-	1	-
S_u (kPa)	20	90	1	300	1
ϕ (°)	-	-	35.8	-	36.2
v	-	-	0.3	-	0.3
v_{ur}	0.2	0.2	-	0.2	-
p_{ref} (kPa)	100	65	-	65	-
SPT-N (blow/ft)	-	-	45	60	70
R_{int}	0.9	0.5	0.6	0.3	0.6

Note: γ = unit weight; E_{50}^{ref} = reference secant stiffness; E_{oed}^{ref} = reference oedometer stiffness; E_{ur}^{ref} = reference unloading-reloading stiffness; E' = effective Young's modulus; m = power for stress-level dependency of stiffness in the HS model; S_u = undrained shear strength; ϕ = effective friction angle; v = Poisson's ratio; v_{ur} = unloading-reloading Poisson's ratio; p_{ref} = reference stress; SPT-N = standard penetration test blow count; R_{int} = interface strength reduction factor.

Table 5. Bored pile properties used in FEM analyses

Pile type	Unit weight, γ (kN/m³)	Poisson's ratio, v	Young's modulus, E (kPa)	Material model	Drainage condition
Bored pile	24	0.2	$2.6\text{x}10^7$	Linear elastic	Non-porous

4.2 Soil Profile and Material Properties

The soil profile adopted in the numerical analyses represented a typical Bangkok subsoil stratigraphy used in foundation design for large buildings. It consisted of five main layers: soft clay, stiff clay, first sand, hard clay, and second sand, extending to a depth of approximately 55 m below ground level.

The clay layers were modelled using the Hardening Soil (HS) model under undrained B conditions to represent short-term response, while the sand layers were modelled as drained materials using the Mohr-Coulomb (MC) model. The HS model was adopted because calibrated HS parameters for Bangkok subsoil are more readily available than the additional small-strain parameters required for the HS-Small model. This modelling scheme reflects the clay-dominated Bangkok profile, where pile-soil-pile interaction is strongly influenced by the low stiffness and high compressibility of the upper soft clay layer. The groundwater table was assigned at the ground surface. Initial effective stresses were generated using the K_0 procedure in PLAXIS 3D, with OCR = 1.0 adopted for the representative normally consolidated Bangkok clay profile. Accordingly, K_0 was automatically generated using $K_0 = 1 - \sin\phi$. Since consolidation and seepage were outside the scope of this study, permeability was not treated as a governing input parameter.

Material parameters for the soil layers were derived from published Bangkok subsoil studies based on regional site investigation databases [23] and earlier finite element applications for Bangkok foundation problems [5]. The HS stiffness parameters were adopted from the framework of Masanou and Amornfa [24], in which representative Bangkok subsoil parameters were refined and adapted for use with the HS model. In that framework, E_{50}^{ref}/S_u was taken as approximately 500 for soft clay and 2,000 for stiff to hard clay. In addition, E_{oed}^{ref} was taken equal to E_{50}^{ref}, and E_{ur}^{ref} was taken as three times E_{50}^{ref}. These relationships provide stiffness parameters consistent with the S_u values adopted for the clay layers.

All soil parameters were kept constant throughout the parametric study to isolate the effects of pile number and spacing ratio under a consistent representative Bangkok subsoil condition. Although spatial variability may affect absolute pile capacity and load–settlement behavior, the present study focuses on normalized group efficiency obtained using the same soil profile and interpretation procedure. The influence of soil heterogeneity on the proposed correction factor should be further examined when site-specific pile-group data become available. The adopted soil parameters are summarized in Table 4.

4.3 Pile Modeling, Geometry, and Boundary Conditions

The bored piles were modelled explicitly as three-dimensional solid volume elements embedded within the soil continuum, rather than as embedded beam elements. Each pile was idealized as a linear elastic, non-porous material representing the cast-in-place reinforced concrete bored piles commonly used in Bangkok. This assumption was adopted because the study focused on geotechnical pile–soil–pile interaction rather than structural failure or cracking of the reinforced-concrete pile section. This modelling approach allowed the soil between adjacent piles to be represented with its actual geometric spacing, which is important for capturing pile-soil-pile interactions in closely spaced pile groups. The pile material properties used in the analyses are summarized in Table 5.

Pile-soil interaction was simulated using interface elements along the pile shaft and base to allow relative displacement between the pile and the surrounding soil. Interface reduction factors were assigned according to the adjacent soil layer to represent reduced shear transfer at the pile–soil interface. The adopted R_{int} values followed previous Bangkok bored-pile numerical studies summarized by Amornfa, Phienwej and Kitpayuck [5]. To examine the influence of the selected interface factors, an additional sensitivity check was performed for a representative nine-pile group, D = 1.0 m, L = 46 m, n = 9, and s/D = 3, together with the corresponding single-pile models. Three cases were considered: the base R_{int} values, values reduced by 20%, and values increased by 20% with an upper limit of 1.0. The interpreted η was 0.764 for all three cases, indicating that the normalized group efficiency for this representative case was not sensitive to the selected R_{int} values within the examined range.

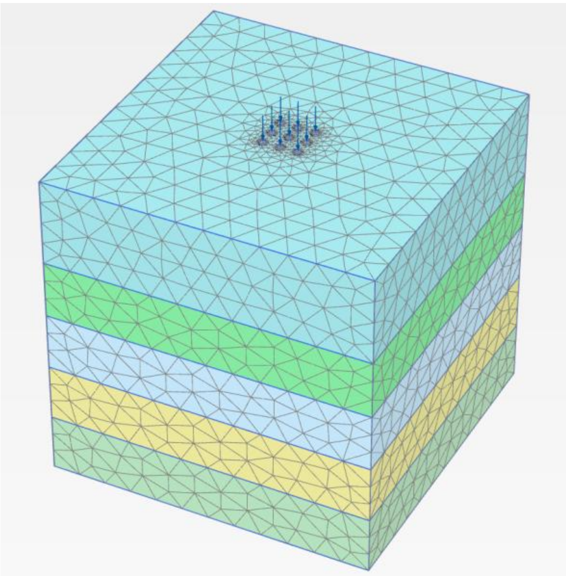

Fig.2 FEM mesh for a representative nine-pile group model.

The numerical domain was defined to minimize boundary effects on the pile-group response. A minimum plan dimension of approximately 50 m × 50 m was used for the single-pile models, while larger domains were adopted for pile-group cases according to group size and spacing. The lateral boundaries were placed sufficiently far from the outermost piles, and the computed stress and deformation contours confirmed that the major deformation zone did not extend to the model boundaries. The finite element mesh was generated using the medium global coarseness option in PLAXIS 3D, with automatic local refinement around the pile–soil interfaces and pile bases, where relatively large stress gradients and pile–soil interaction were expected. A representative mesh for the nine-pile group model is shown in Fig.2. Similar boundary checks and local mesh refinement procedures have also been adopted in geotechnical FEM studies [25]. The lateral boundaries were constrained in the normal direction while allowing tangential movement, and the bottom boundary was fixed in all directions. Each pile in the group was modelled individually, allowing the responses for corner, edge, and center piles to be represented consistently across all cases.

4.4 Loading Procedure and Definition of Group Efficiency

Vertical loading was applied at the pile heads in a load-controlled manner using incremental load steps. For all numerical cases, the load increment was defined as 0.1 of the single-pile ultimate capacity calculated in advance using a conventional static capacity formula. This value was used only to define the load-step magnitude and was not used in the subsequent calculation of pile-group efficiency. At each loading step, equal vertical loads were applied simultaneously to all pile heads in the group, and loading was continued until failure behavior was observed in the load-settlement response. This standardized head-loading condition was adopted to define capacity-based group efficiency and to allow direct comparison with classical pile-group efficiency equations. Pile cap stiffness, raft-soil contact, and nonuniform superstructure loading were not included so that the effects of pile-soil-pile interaction due to pile number and spacing ratio could be isolated. The load-controlled increments were used to obtain monotonic load-settlement responses for capacity interpretation; post-peak softening was not the primary focus of this study.

The ultimate capacities of both single piles and pile groups were interpreted from the computed load-settlement curves using graphical extrapolation methods. The Chin method was adopted as the primary interpretation technique because it linearizes the load-settlement relationship and provides an objective estimate of ultimate capacity for nonlinear friction-pile behavior [26]. In addition, the Mazurkiewicz method was used as an independent graphical check to verify the consistency of the interpreted capacities [27]. For all efficiency calculations, the Chin-derived ultimate capacities were used. A fixed settlement criterion, such as 10% of pile diameter, was not adopted as the primary failure criterion because the objective was to maintain a capacity-based interpretation consistent with classical pile-group efficiency equations.

The FEM-derived pile-group efficiency, η_{FEM}, was defined consistently from the FEM-derived ultimate capacities as

$$\eta_{FEM} = \frac{Q_g}{nQ_s} \quad (2)$$

where Q_g is the ultimate capacity of the pile group interpreted from the FEM load-settlement curve, Q_s is the ultimate capacity of the corresponding single pile interpreted using the same method, and n is the total number of piles in the group.

This definition ensured that single-pile and pile-group capacities were evaluated under the same modelling assumptions and interpretation procedure. Therefore, η_{FEM} represents the relative influence of pile-soil-pile interaction in Bangkok subsoil, rather than an exact prediction of absolute axial pile capacity.

4.5 Single-Pile Field Benchmark

A single-pile field benchmark was added to check the reasonableness of the numerical load–settlement response. The benchmark was based on the static load test of a 1.65 m diameter and 60 m long bored pile in Bangkok subsoil reported by Amornfa [28]. This case was selected because measured load–settlement data, soil profile, and project-specific soil parameters were available. The benchmark was reanalysed using the current PLAXIS 3D framework, with clay and sand layers modelled consistently with the main parametric analyses. The pile was idealized as a linear elastic, non-porous reinforced-concrete material.

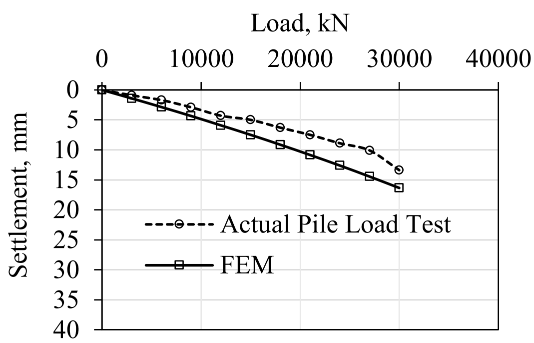

Fig.3 Measured and computed load-settlement responses of the benchmark pile

Fig.3 compares the measured and computed load–settlement responses. At loads of 15,000 and

30,000 kN, the computed pile-head settlements were 7.49 and 16.35 mm, compared with measured settlements of 5.0 and 13.4 mm, respectively. The FEM slightly overpredicted the measured settlement and therefore provided a conservative representation of the single-pile response. This benchmark was used only to check the numerical framework for a single bored pile in Bangkok subsoil and was not used to recalibrate the proposed group-efficiency correction factor.

5. RESULTS AND DISCUSSION

5.1 General Behavior of Group Pile Efficiency

The general behavior of the FEM-derived pile-group efficiency, η_{FEM} is presented in Figs.4 and 5, with representative values summarized in Table 6. Based on these results, η_{FEM} was consistently lower than unity for both bored pile series, indicating that the axial capacity of a pile group was smaller than the sum of the corresponding single-pile capacities. This behavior reflects pile-soil-pile interaction in Bangkok subsoil, where overlapping stress and displacement fields reduced the contribution of individual piles.

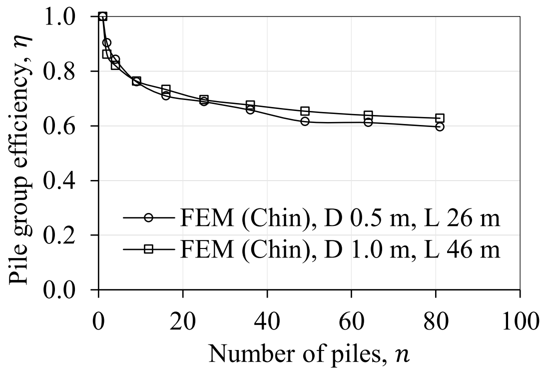

Fig.4 Effect of pile number on FEM-derived pile-group efficiency

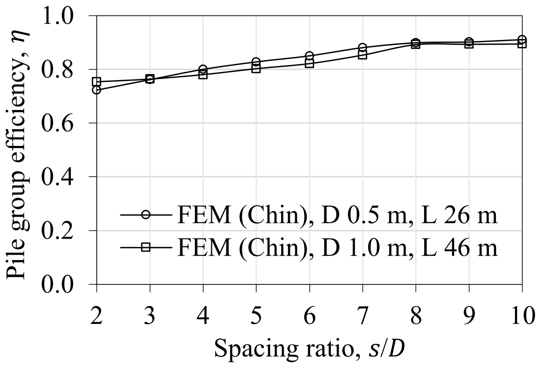

Fig.5 Effect of spacing ratio on FEM-derived pile-group efficiency for nine-pile groups

As shown in Fig.4, η_{FEM} decreased as the number of piles increased at a constant spacing ratio of s/D = 3. The reduction was more pronounced from small-to-medium group sizes and became more gradual for larger groups. This indicated that group interaction developed progressively as additional piles were introduced; however, the rate of efficiency reduction decreased for larger pile groups. The two pile series showed broadly similar trends, suggesting that the effect of group size was consistent for the investigated pile dimensions and penetration depths.

Fig.5 shows the effect of the spacing ratio on the nine-pile groups. In contrast to the pile-number series, η_{FEM} increased as s/D increased. At close spacing, the piles behaved as a strongly interacting system, resulting in lower efficiency. As spacing increased, the overlap of stress and displacement fields decreased, and the response of each pile became closer to that of an isolated pile. The increase in efficiency was more evident at low spacing ratios and became flatter at larger s/D, indicating that additional spacing beyond a moderate range provided progressively smaller improvement.

These trends are consistent with the pile-group interaction concept of Poulos and Davis [3], in which overlapping stress and displacement fields reduce the mobilized resistance of individual piles. Similar effects of spacing and pile number have also been reported in numerical studies of pile groups in soft clay and stratified soils [11, 12].

Table 6. Representative FEM-derived pile-group efficiencies

D (m)	L (m)	n	s/D	η_{FEM} (Mazurkiewicz)	η_{FEM} (Chin)
0.5	26	2	3	0.891	0.904
0.5	26	9	3	0.766	0.762
0.5	26	25	3	0.683	0.689
0.5	26	81	3	0.584	0.597
1.0	46	2	3	0.862	0.862
1.0	46	9	3	0.743	0.764
1.0	46	25	3	0.648	0.696
1.0	46	81	3	0.628	0.628
0.5	26	9	2	0.723	0.723
0.5	26	9	3	0.766	0.762
0.5	26	9	5	0.838	0.828
0.5	26	9	10	0.993	0.911
1.0	46	9	2	0.726	0.754
1.0	46	9	3	0.743	0.764
1.0	46	9	5	0.811	0.803
1.0	46	9	10	0.991	0.895

The numerical values in Table 6 support these trends. At s/D = 3, η_{FEM} decreased with increasing pile number, while for the nine-pile groups, η_{FEM} increased with an increasing spacing ratio. Overall, based on these FEM results, pile-group efficiency in Bangkok subsoil was not a constant parameter, but a variable response controlled mainly by group size and pile spacing. These findings provided the basis for comparison with classical efficiency equations in the following section.

The Chin and Mazurkiewicz interpretations were generally consistent for most cases. In the spacing-ratio series, the differences in η_{FEM} were small for s/D = 2–5 but became more noticeable at s/D = 10, where the Mazurkiewicz values were 0.993 and 0.991, compared with Chin-derived values of 0.911 and 0.895 for the small and large pile series, respectively. For consistency, the Chin-derived capacities were retained for all subsequent efficiency and error calculations.

5.2 Comparison with Classical Methods and Error Analysis

The FEM-derived pile-group efficiencies were compared with classical capacity-based efficiency equations to evaluate their applicability to bored pile groups in Bangkok subsoil. The Chin-derived FEM results, η_{FEM}, were used as the reference values. The comparisons for pile-number variation and spacing-ratio variation are shown in Figs.6 and 7 and summarized in Tables 7 and 8.

Fig.6 and Table 7 compare the results for varying numbers of piles at a constant spacing ratio of s/D = 3. Based on these FEM results, there was a gradual decrease in efficiency as the number of piles increased; this trend was also captured by both classical methods. However generally, the Converse-Labarre method produced values closer to the FEM results than the Feld method. For the pile-number series, Converse-Labarre slightly underestimated the FEM values for smaller groups in several cases, while its predictions became closer to or slightly higher than the FEM results for larger groups. The Feld method also followed the decreasing trend, but generally gave lower values than FEM, particularly for the larger pile series.

Fig.7 and Table 8 show the comparison for the nine-pile groups among varying spacing ratios. In this series, η_{FEM} increased with increasing s/D. The Converse-Labarre method reproduced this spacing-dependent trend reasonably well, although it underestimated the FEM results at close spacing, especially at s/D = 2 and 3. For s/D > 3, the Converse-Labarre predictions became much closer to the FEM values. In contrast, the Feld method produced a constant efficiency value over the full spacing range and therefore could not represent an increase in efficiency with spacing. This led to increasing underestimation at larger spacing ratios.

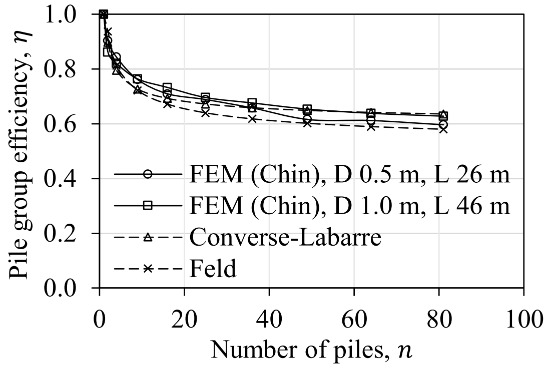

Fig.6 Comparison of efficiency methods for pile-number variation

Table 7. Efficiency comparison for pile-number variation at s/D = 3

n	η_{CL} Converse-Labarre	η_{FELD} Feld	η_{FEM} (Chin), D = 0.5 m, L = 26 m	η_{FEM} (Chin), D = 1.0 m, L = 46 m
1	1.000	1.000	1.000	1.000
2	0.898	0.938	0.904	0.862
4	0.795	0.813	0.844	0.821
9	0.727	0.722	0.762	0.764
16	0.693	0.672	0.710	0.733
25	0.672	0.640	0.689	0.696
36	0.659	0.618	0.658	0.676
49	0.649	0.602	0.616	0.654
64	0.642	0.590	0.612	0.639
81	0.636	0.580	0.597	0.628

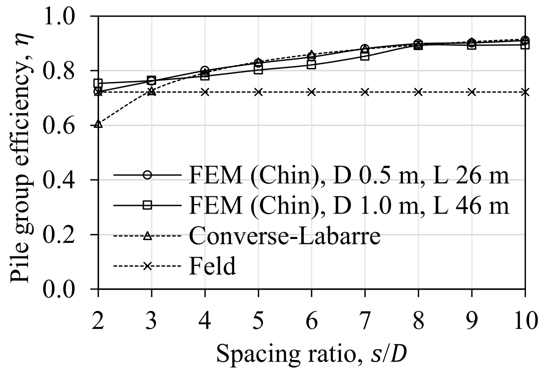

Fig.7 Comparison of efficiency methods for spacing-ratio variation

Table 8. Efficiency comparison for spacing-ratio variation in nine-pile groups

s/D	η_{CL} Converse-Labarre	η_{FELD} Feld	η_{FEM} (Chin), D = 0.5 m, L = 26 m	η_{FEM} (Chin), D = 1.0 m, L = 46 m
2	0.606	0.722	0.723	0.754
3	0.727	0.722	0.762	0.764
4	0.792	0.722	0.800	0.780
5	0.832	0.722	0.828	0.803
6	0.860	0.722	0.850	0.822
7	0.880	0.722	0.881	0.853
8	0.894	0.722	0.899	0.893
9	0.906	0.722	0.902	0.894
10	0.915	0.722	0.911	0.895

To quantify the deviations, percentage errors were calculated relative to η_{FEM} as:

$$Error(\%) = \frac{\eta_{method} - \eta_{FEM}}{\eta_{FEM}} \times 100 \quad (3)$$

where η_{method} represents the efficiency predicted by either the Converse-Labarre or Feld method.

The mean signed error was used to indicate the direction of bias, while the mean absolute error was used to evaluate the magnitude of the prediction error. Range-dependent bias was identified based on dividing the pile-number series into a lower range of n =2–25 and an upper range of n = 36–81. The spacing-ratio series was divided into a lower range of s/D = 2–3 and an upper range of s/D = 4–10. The resulting error statistics are summarized in Table 9.

The error statistics supported the selection of the Converse-Labarre equation as the main basis for local modification in the pile-number series. The mean absolute errors of Converse-Labarre were 3.62% and 2.89% for the smaller and larger pile series, respectively, compared to 4.42% and 7.03%, respectively, for Feld, indicating that Converse-Labarre provided a closer estimate when the number of piles was varied. However, the range-based signed errors showed that its bias was not uniform across group size. For the smaller pile series, the signed error changed from -3.17% in the lower range to +4.18% in the upper range, indicating a shift from slight underestimation to slight overestimation. For the larger pile series, the corresponding values changed from -2.54% to -0.41%, showing that the bias decreased as the group size increased.

For the spacing-ratio series, the difference between the two methods was more pronounced. Converse-Labarre produced mean absolute errors of 2.77% and 4.58% for the smaller and larger pile series, whereas the spacing-independent Feld method produced errors of 13.45% and 12.46%, respectively. The main weakness of Converse-Labarre occurred at close spacing, where the mean signed errors were -10.32% and -12.19% for the smaller and larger pile series, respectively, when s/D = 2–3. In contrast, the errors became smaller in the upper spacing range, with signed errors of +0.15% and +2.41% for the smaller and larger pile series, respectively, when s/D = 4–10. The Feld method systematically underestimated at larger spacing ratios because its prediction did not vary with s/D.

Table 9. Error statistics of classical efficiency methods relative to FEM

Case series	Pile series	Method	Mean signed error (%)	Mean absolute error (%)	Signed error, lower range (%)	Signed error, upper range (%)	Maximum absolute error (%)
Pile-number series	D0.5–L26	Converse-Labarre	0.14	3.62	-3.17	4.18	6.55
		Feld	-3.60	4.42	-2.96	-3.70	7.08
	D1.0–L46	Converse-Labarre	-1.59	2.89	-2.54	-0.41	5.47
		Feld	-5.09	7.03	-2.82	-7.94	8.73
Spacing-ratio series	D0.5–L26	Converse-Labarre	-2.18	2.77	-10.32	0.15	16.09
		Feld	-13.45	13.45	-2.62	-16.55	20.70
	D1.0–L46	Converse-Labarre	-0.84	4.58	-12.19	2.41	19.53
		Feld	-12.46	12.46	-4.81	-14.64	19.30

Overall, the comparison supported the use of the Converse-Labarre equation as the basis for local modification. Although Converse-Labarre still showed systematic bias, particularly at close spacing, it captured the main effects of both the pile number and spacing ratio. The Feld method was retained only as a simple classical benchmark because its spacing-independent formulation does not provide a suitable basis for developing a spacing-sensitive correction. These findings supported the development of a Bangkok-specific correction factor based on the Converse-Labarre equation in the following section.

6. DEVELOPMENT OF CORRECTION FACTOR FOR BANGKOK SOFT CLAY

6.1 Rationale for Modifying the Converse-Labarre Equation

The results in Section 5 show that the Converse-Labarre equation provided a reasonable basis for local modification because it captured the effects of both pile number and spacing ratio. In addition, the Converse–Labarre equation is commonly used and well recognized in routine pile-foundation design practice in Thailand because of its simple geometric form and direct use of pile spacing and group arrangement. Although the Feld method was included as a simple classical benchmark, its spacing-independent formulation does not provide a suitable basis for developing a spacing-sensitive correction. Therefore, the proposed modification was developed from the Converse-Labarre equation.

Specifically, the Converse-Labarre equation reproduced the decrease in efficiency with an increasing number of piles and the increase in efficiency with an increasing spacing ratio. However, systematic bias remained in specific ranges. In particular, Converse-Labarre tended to underestimate η_{FEM} at close spacing, especially for s/D = 2 to 3, while its predictions became much closer to the FEM results at larger spacing ratios. For the pile-number series, the overall bias was smaller, although the direction of error varied with group size.

Based on these results, the limitation of Converse-Labarre was mainly related to prediction magnitude, rather than the inability to capture the governing trend. A local correction factor is required for Bangkok subsoil since the equation is primarily geometric and does not explicitly include soil stiffness, stress redistribution, nonlinear deformation, or the compressibility of soft clay. Therefore, the present study adopted a multiplicative correction factor applied to the original Converse-Labarre efficiency, allowing the corrected equation to retain the simplicity of the classical method, while improving agreement with FEM-derived efficiencies.

6.2 Correction Framework and Proposed Equation

A multiplicative correction framework was adopted to improve the applicability of the Converse-Labarre equation to Bangkok subsoil, while preserving its practical form. The corrected pile-group efficiency is expressed as:

$$\eta_{BKK} = C_{BKK}\eta_{CL} \tag{4}$$

where η_{CL} is the efficiency predicted by the original Converse-Labarre equation and C_{BKK} is the Bangkok-specific correction factor.

The correction factor was calculated from the FEM results as:

$$C_{BKK} = \frac{\eta_{FEM}}{\eta_{CL}} \tag{5}$$

where η_{FEM} is the FEM-derived efficiency interpreted using the Chin method.

Thus, C_{BKK} = 1.0 indicates no correction, whereas values greater or less than unity indicate underestimation or overestimation, respectively, by the original Converse-Labarre equation.

The calculated C_{BKK} values are shown in Figs.8 and 9. For the pile-number series, the correction factor remained close to unity over most of the range, confirming that Converse-Labarre already approximated the FEM results reasonably well. For the spacing-ratio series, C_{BKK} was higher at close spacing and decreased toward unity as s/D increased, indicating that the main correction demand occurs for closely spaced pile groups.

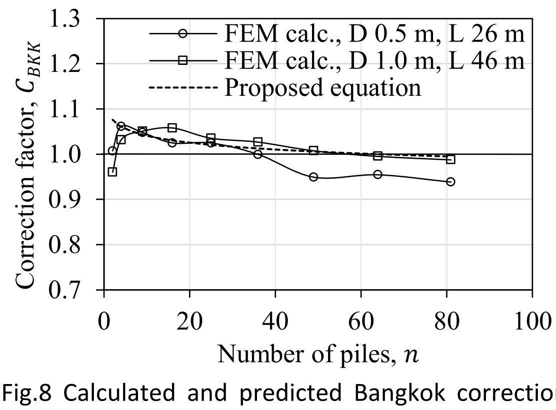

Fig.8 Calculated and predicted Bangkok correction factor for pile-number variation

Table 10. Candidate regression models for C_{BKK}

Model	Equation form	Regression variables	R^2	Mean absolute error (%)	Maximum absolute error (%)	Decision
Model 1	$C_{BKK} = a+b\ln(n)+c\ln(s/D)$	ln(*n*), ln(*s*/*D*)	0.336	3.02	13.73	Not selected
Model 2	$C_{BKK} = a+b\ln(n)+c/(s/D)$	ln(*n*), 1/(*s*/*D*)	0.480	3.34	10.83	Not selected
Model 3	$C_{BKK} = a+b\ln(n)+cI_{close}$	ln(*n*), I_{close}	0.246	2.67	15.92	Not selected
Model 4	$C_{BKK} = a+b\ln(n)+c/\ln(s/D)$	ln(*n*), 1/ln(*s*/*D*)	0.587	2.61	12.03	Selected

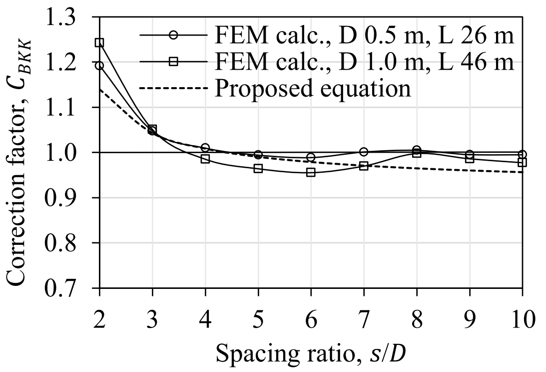

Fig.9 Calculated and predicted Bangkok correction factor for spacing-ratio variation

Four candidate regression models were examined to represent C_{BKK}, as summarized in Table 10. In all these models, group size was represented by ln(*n*), while the spacing effect was introduced using alternative terms: ln(*s*/*D*), 1/(*s*/*D*), a close-spacing indicator I_{close}, and 1/ln(*s*/*D*). The indicator I_{close} was defined as 1 for $s/D \leq 3$ and 0 for $s/D > 3$. The objective was to identify a simple regression form that could capture the main FEM-derived correction trend.

Among the four models, Model 4 was selected because it provided the highest coefficient of determination (R^2 = 0.587) and the lowest mean absolute error after correction (2.61%). Although Model 2 had the lowest maximum absolute error, Model 4 was selected based not only on R^2, but also on its overall balance between error reduction, simplicity, physical interpretability, and consistency with the variables used in the original Converse-Labarre equation. In addition, the reciprocal logarithmic spacing term reflected the strong correction required at close spacing and the gradual convergence toward unity at larger spacing ratios. The selected Bangkok correction factor could be expressed as:

$$C_{BKK} = a + b\ln(n) + \frac{c}{\ln(s/D)} \quad (6)$$

where *a*, *b* and *c* are regression coefficients.

Table 11. Regression coefficients of selected correction model

Parameter	Value	Description
a	0.92612	Intercept
b	-0.02192	Coefficient of ln(*n*)
c	0.18144	Coefficient of 1/ln(*s*/*D*)
R^2	0.587	Coefficient of determination

Based on the fitted coefficients in Table 11, the proposed best-estimate correction factor was:

$$C_{BKK} = 0.92612 - 0.02192\ln(n) + \frac{0.18144}{\ln(s/D)} \quad (7)$$

and the corrected pile-group efficiency was then obtained from Eq. (4).

Additionally, a lower-bound conservative form was developed for design situations requiring a more cautious estimate. The conservative correction factor was defined by shifting the best-estimate equation downward by one residual standard deviation:

$$C_{BKK,cons} = C_{BKK} - ks_e \quad (8)$$

where C_{BKK} is the best-estimate correction factor obtained from Eq. (7), s_e is the residual standard deviation, and *k* is a conservatism factor.

In the present study, k = 1.0 and s_e = 0.0396 were adopted to define an empirical lower-bound correction based on residual scatter. The value of *k* is not a reliability-based resistance factor and should not replace code-based partial factors or project-specific reliability requirements. The corresponding conservative efficiency is:

$$\eta_{BKK,cons} = C_{BKK,cons}\eta_{CL} \quad (9)$$

The fitted best-estimate equation is plotted with the calculated C_{BKK} values in Figs.8 and 9. The equation captures the principal correction trends for both parametric series: a near-unity correction for most pile-number cases and a higher correction demand at close spacing. Therefore, the proposed framework retains the simplicity of the Converse-Labarre equation, while incorporating the local subsoil effects identified from the FEM analyses. The performance of the best-estimate and conservative forms is evaluated in the following section.

6.3 Performance Evaluation and Applicability Range

The performance of the proposed Bangkok correction equations was evaluated by comparing the original Converse-Labarre prediction, the best-estimate equation, and the conservative equation with the FEM-derived pile-group efficiency values. The comparison was based on values for the mean signed error, mean absolute error, and maximum absolute error, as summarized in Table 12. The relationship between predicted and FEM-derived efficiency values is shown in Fig.10.

Table 12. Error statistics before and after Bangkok correction

Method	Mean signed error (%)	Mean absolute error (%)	Maximum absolute error (%)
Converse-Labarre	-1.13	3.46	19.53
Best-estimate equation	0.13	2.61	12.03
Conservative equation	-3.78	4.62	11.47

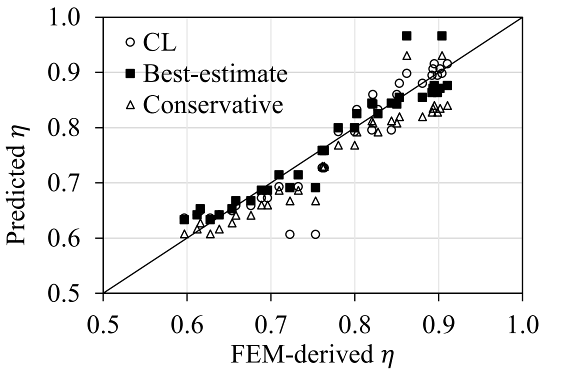

Fig.10 Predicted versus FEM-derived pile-group efficiency before and after correction; the straight line represents the 1:1 agreement line

The best-estimate equation improved the overall prediction performance relative to the original Converse-Labarre equation. The mean signed error changed from -1.13% to 0.13%, indicating that the overall bias was nearly eliminated. The mean absolute error decreased from 3.46% to 2.61%, while the maximum absolute error was reduced from 19.53% to 12.03%. This improvement should be interpreted as a local refinement of the original Converse-Labarre equation rather than as a replacement for the classical method, which already showed reasonably close agreement with the FEM results. The proposed correction provides a simple adjustment for Bangkok bored pile groups, and the reduction in maximum absolute error indicates that it is mainly useful for reducing larger deviations while preserving the practical form of the original equation.

The conservative equation provided more cautious estimates of pile-group efficiency, as intended. Its mean signed error was -3.78%, indicating a downward shift relative to the best-estimate equation. Although its mean absolute error increased to 4.62%, the maximum absolute error decreased slightly to 11.47%. In the calibration dataset, the conservative form achieved a coverage ratio of 86.11%, meaning that 86.11% of the FEM-derived cases remained above the conservative prediction. Therefore, the conservative equation may be used when a cautious estimate is preferred, although it should not be interpreted as a guaranteed lower bound for all possible configurations.

Fig.10 supports the same interpretation. The original Converse-Labarre predictions had a wider spread around the 1:1 line, whereas the best-estimate equation produced predictions more closely clustered around the FEM-derived values. The conservative equation shifted most points below the 1:1 line, consistent with its intended lower-bound role.

The proposed equations should be applied within the calibration range and modelling assumptions of the present study. The dataset consisted of two parametric series: pile-number variation of n = 2–81 at s/D = 3, and spacing-ratio variation at s/D = 2–10 for the nine-pile groups. The term $1/\ln(s/D)$ limits the proposed equation to the calibrated range of s/D = 2–10 and should not be extrapolated toward s/D = 1.0. Although spacing ratios up to s/D = 10 were included, predictions at large spacing ratios should be regarded mainly as numerical trend confirmation because practical layouts are commonly governed by smaller spacing ratios.

The equations are intended for bored pile groups in Bangkok subsoil represented by the adopted soil profile, constitutive models, and pile series. The proposed equations were calibrated using regular and symmetrical pile arrangements only. Irregular pile layouts, asymmetric spacing, and pile arrangements governed by shear-wall or core-wall locations were not directly considered and should be evaluated using project-specific numerical analysis. Application to other untested combinations of n and s/D should be regarded as model-based preliminary estimation rather than direct validation. Application outside the calibration ranges should be considered extrapolation and should be supported by additional verification when design sensitivity is high. In particular, pile groups larger than n = 81 were not directly simulated; although the FEM results showed a relatively small change in efficiency for large pile groups, this trend was represented empirically through the ln(n) term in the proposed correction model and should not be over-extrapolated. The proposed equation was calibrated and evaluated using the same FEM dataset; therefore, its predictive performance should be interpreted as calibration performance rather than validation against an independent dataset. Additional FEM cases or field pile-group load-test data are required for independent validation in future studies.

The proposed correction factor addresses capacity-based group efficiency only; long-term consolidation, time-dependent effective-stress changes, and serviceability settlement in Bangkok soft clay should be assessed separately in practical foundation design. The piles were idealized as wished-in-place elements; therefore, construction-induced effects such as stress relief during borehole excavation, slurry support, and concrete placement were not explicitly simulated. The proposed correction factor applies to head-loaded pile groups without explicit pile-cap or raft-soil interaction; capped or piled-raft systems require separate assessment of load sharing.

Overall, the proposed Bangkok correction framework improves the practical estimation of pile-group efficiency while maintaining the simplicity of the Converse-Labarre equation. In practice, engineers may apply the correction in three steps: (1) calculate the original Converse-Labarre efficiency for the selected pile arrangement; (2) compute the Bangkok correction factor using the proposed equation within the calibrated range; and (3) obtain the corrected efficiency for preliminary comparison of alternative pile layouts. The best-estimate form is suitable for comparative assessment, whereas the conservative form provides an additional design-oriented option when a lower-bound estimate is preferred. However, the corrected efficiency should be used together with conventional geotechnical design checks, including factor of safety, settlement assessment, pile-cap or raft interaction, and project-specific site investigation data. Additional field validation using full-scale pile-group load tests or reliable monitoring data is still required before broader generalization.

7. CONCLUSIONS

This study confirmed that the Converse-Labarre equation provides a reasonable classical basis for estimating bored pile-group efficiency in Bangkok subsoil when compared with three-dimensional FEM results. Two representative bored pile series were considered: a smaller pile series terminating in the first sand layer and a larger pile series extending to the second sand layer. Ultimate capacities from FEM load-settlement curves were interpreted mainly using the Chin method, with the Mazurkiewicz method used as an independent graphical check.

The FEM results showed that pile-group efficiency in Bangkok subsoil was consistently lower than unity, confirming the importance of pile-soil-pile interaction in soft clay. Efficiency decreased as the number of piles increased and increased as the spacing ratio increased. These trends indicate that pile-group efficiency should not be treated as a constant value, especially for closely spaced pile groups.

Comparison with classical capacity-based methods showed that the Converse-Labarre equation captured both group-size and spacing effects and was therefore suitable as the basis for local modification. However, systematic bias remained, particularly at close spacing ratios, indicating the need for a Bangkok-specific correction factor.

A Bangkok-specific correction factor was developed using a multiplicative correction applied to the original Converse–Labarre efficiency. The selected model, based on ln(n) and 1/ln(s/D), reduced the mean signed error from -1.13% to 0.13%, the mean absolute error from 3.46% to 2.61%, and the maximum absolute error from 19.53% to 12.03%. These results show that the proposed correction mainly improves the original equation by reducing bias and larger deviations while preserving its simple practical form.

The proposed correction framework improves the local application of the Converse-Labarre equation for bored pile groups in Bangkok subsoil. However, its use should be limited to the calibration range and modelling assumptions of the present study. Future work should include additional pile configurations, wider combinations of *n* and *s*/*D*, different Bangkok subsoil profiles, and validation against full-scale pile-group load tests or reliable field monitoring data.

8. ACKNOWLEDGMENTS

The authors gratefully acknowledge the Department of Civil Engineering, Faculty of Engineering at Kamphaeng Saen, Kasetsart University, for providing research facilities and access to the licensed PLAXIS 3D software used in this study. The authors thank the Kasetsart University Research and Development Institute, Kasetsart University, for supporting the English language editing. The assistance of students from the Department of Civil Engineering in conducting PLAXIS 3D analyses and preparing preliminary results is also appreciated.

9. REFERENCES

1. Bolin, H.W., The Pile Efficiency Formula of the Uniform Building Code, Building Standards Monthly, 1941, 10(1), pp. 4–5.
2. American Society of Civil Engineers, Standard Guidelines for the Design and Installation of Pile Foundations, ASCE 20-96, American Society of Civil Engineers, New York, 1997, pp. 1–29.
3. Poulos, H.G. and Davis, E.H., Pile Foundation Analysis and Design, John Wiley & Sons, New York, 1980, pp. 1–397.
4. Yudiawati, Y., Mochtar, I.B., and Mochtar, N.E., Group Capacity and Efficiency of Full Friction Piles on Very Soft Soil, International Journal of GEOMATE, 2019, 16(57), pp. 201–208. https://doi.org/10.21660/2019.57.68950
5. Amornfa, K., Phienwej, N., and Kitpayuck, P., Current Practice on Foundation Design of High-Rise Buildings in Bangkok, Thailand, Lowland Technology International, 2012, 14(2), pp. 70–83.
6. Suzuki, N. and Seki, T., Vertical Load Test and Settlement Analysis of Cast-In-Place Concrete Nodular Piles Supporting a High-Rise Building, Geotechnical Engineering Journal of the SEAGS & AGSSEA, 2011, 42(2), pp. 20–28.
7. Amornfa, K. and Sa-nguanduan, N., Load-Displacement Behavior of Single Pile in Sand Using Physical Model Test and Finite Element Method, International Journal of GEOMATE, 2023, 24(103), pp. 68–75. https://doi.org/10.21660/2023.103.3718
8. Pratama, G.A.P., Amornfa, K., Mairaing, W., and Soralump, S., Investigation of Differential Settlement of Pagoda Foundation using 3D Finite Element Method, International Journal of GEOMATE, 2024, 26(113), pp. 10–18. https://doi.org/10.21660/2024.113.4005
9. Amornfa, K., Quang, H.T., and Tuan, T.V., 3D Numerical Analysis of Piled Raft Foundation for Ho Chi Minh City Subsoil Conditions, Geomechanics and Engineering, 2022, 29(2), pp. 183–192. https://doi.org/10.12989/gae.2022.29.2.183
10. Pratama, G.A.P., Amornfa, K., Mairaing, W., and Soralump, S., Analysis of Complex Foundation on Historical Pagoda in Thailand using 3D Finite Element Method, International Journal of GEOMATE, 2022, 23(98), pp. 125–135. https://doi.org/10.21660/2022.98.3585
11. Ferchat, A., Houhou, M.N., and Benmebarek, S., Numerical Investigation on Pile Group Efficiency Embedded in Soft Clay, World Journal of Engineering, 2021, 18(3), pp. 397–406. https://doi.org/10.1108/WJE-04-2020-0112
12. Pratama, I.T., Widjaja, B., and Budianto, K.A., Numerical Study on Pile Group Efficiency for Piles Embedded in Cohesive and Cohesionless Soils, E3S Web of Conferences, 2023, 429(04003), pp. 1–9. https://doi.org/10.1051/e3sconf/202342904003
13. Feld, J., Discussion on Friction Pile Foundations, Transactions of the American Society of Civil Engineers, 1943, 108(1), pp. 143–144.
14. Whitaker, T., Experiments with Model Piles in Groups, Géotechnique, 1957, 7(4), pp. 147–167. https://doi.org/10.1680/geot.1957.7.4.147
15. Seiler, J.F. and Keeney, W.D., The Efficiency of Piles in Groups, Wood Preserving News, 1944, 22(11), pp. 109–118.
16. Sayed, S.M. and Bakeer, R.M., Efficiency Formula for Pile Groups, Journal of Geotechnical Engineering, 1992, 118(2), pp. 278–299. https://doi.org/10.1061/(ASCE)0733-9410(1992)118:2(278)
17. Hanna, A.M., Morcous, G., and Helmy, M., Efficiency of Pile Groups Installed in Cohesionless Soil using Artificial Neural Networks, Canadian Geotechnical Journal, 2004, 41(6), pp. 1241–1249.

https://doi.org/10.1139/T04-050
18. McCabe, B.A. and Lehane, B.M., Behavior of Axially Loaded Pile Groups Driven in Clayey Silt, Journal of Geotechnical and Geoenvironmental Engineering, 2006, 132(3), pp. 401–410. https://doi.org/10.1061/(ASCE)1090-0241(2006)132:3(401)
19. Ateş, B. and Şadoğlu, E., Experimental Investigation for Group Efficiency of Driven Piles Embedded in Cohesionless Soil, KSCE Journal of Civil Engineering, 2023, 27(12), pp. 5123–5134. https://doi.org/10.1007/s12205-023-1580-0
20. Melchior Filho, J., Bonan, V.H.F., and Moura, A.S., Experimental Study of the Group Effect on the Bearing Capacity of Bored Piles in Sandy Soil, Soils and Rocks, 2020, 43(1), pp. 11–20. https://doi.org/10.28927/SR.431011
21. Asif, T.H., Islam, S., Basak, A., Shahriar, F., and Rahman, S.M.S., Application of Numerical Method in Assessing the Variations in Pile Group Efficiency under Different Circumstances, Computational Engineering and Physical Modeling, 2022, 5(1), pp. 50–68. https://doi.org/10.22115/cepm.2022.324662.1200
22. Zhao, J.N., Zong, Z.L., Huang, Y.H., Jiang, P., Fan, Y.M., and Cen, H., Vertical Bearing Capacity of HSCM Pile Groups in Marine Soft Clay, Marine Georesources and Geotechnology, 2025, 43(8), pp. 1554–1572. https://doi.org/10.1080/1064119X.2024.2419535
23. Amornkul, C., Engineering Subsoil Database of Lower Central Plain, Thailand, Master's Thesis, Kasetsart University, Bangkok, 2010, pp. 1–210.
24. Masanou, P. and Amornfa, K., Prediction Equation of Pile Spring Stiffness for Bored Piles in Bangkok, Journal of Engineering and Innovation, 2022, 15(2), pp. 37–47.
25. Maleki, M., and Mir Mohammad Hosseini, S.M., Assessment of the Pseudo-static Seismic Behavior in the Soil Nail Walls Using Numerical Analysis, Innovative Infrastructure Solutions, 2022, 7, Article 262, pp. 1–18. https://doi.org/10.1007/s41062-022-00861-5
26. Chin, F.K., Estimation of The Ultimate Load of Piles from Tests not Carried to Failure, in Proceedings of the Second Southeast Asian Conference on Soil Engineering, 1970, Singapore City, pp. 81–92.
27. Mazurkiewicz, B.K., Test Loading of Piles According to Polish Regulations, Royal Swedish Academy of Engineering Sciences, Commission on Pile Research, Stockholm, Sweden, 1972, pp. 1–31.
28. Amornfa, K., Analysis of Piled Raft Foundations with Their Application to Bangkok Subsoil Condition, Thailand, Doctoral Dissertation, Asian Institute of Technology, Bangkok, 2012, pp. 1–195.